Supporting Information

NIR-II photoacoustic imaging-guided synergistic cancer therapy with tumor-targeting copper selenide-iron manganese layered double hydroxide nanocomplex

Yanting Yang,[a] Shulong Wang,[*ab] Shengqiang Hu,[a] Yanni Luo,[a] Zongyi He,[a] Shulin Zhao[*a]

[a] State Key Laboratory for Chemistry and Molecular Engineering of Medicinal Resources, Collaborative Innovation Center for Guangxi Ethnic Medicine, School of Chemistry and Pharmaceutical Science, Guangxi Normal University, Guilin 541004, China

[b] Guangxi Key Laboratory of Agricultural Resources Chemistry and Biotechnology, College of Chemistry and Food Science, Yulin Normal University, Yulin 537000, China

*Corresponding author: shulonghs@163.com (S.W.); zhaoshulin001@163.com (S.Z.).

Experimental Section

Materials

Selenium dioxide (SeO_2), hydrazine hydrate ($N_2H_4 \cdot H_2O$), copper chloride dihydrate ($CuCl_2 \cdot 2H_2O$), polyvinylpyrrolidone (PVP), dopamine hydrochloride, manganese chloride tetrahydrate ($MnCl_2 \cdot 4H_2O$), ferric chloride hexahydrate ($FeCl_3 \cdot 6H_2O$), sodium hydroxide (NaOH) were procured from Aladdin Reagent Co. Methoxymercapto polyethylene glycol (mPEG-SH) was sourced from Zhenjun Biological, Shanghai, China. All reagents were of analytical grade and used without further purification.

Instrumentation

Transmission electron microscopy (TEM) images, EDS, and elemental mapping were accomplished using a Talos F200S transmission electron microscope (ThermoFisher Scientific, USA), operating at an accelerating voltage of 200 kV. The powder X-ray diffraction (PXRD) data were collected on a D8 ADVANCE instrument. UV-vis-NIR absorption spectra were obtained using a UV-2600 spectrophotometer (Shimadzu Co., Japan). Both in vitro and in vivo PA imaging were conducted on a multispectral optoacoustic tomography (MSOT) inVision 256-TF scanner (iThera Medical GmbH, Germany). X-ray photoelectron spectroscopy (XPS) analysis was performed on an ESCALAB 250Xi X-ray photoelectron spectrometer (Thermo Fisher Scientific Inc., Waltham, MA, USA). Dynamic light scattering (DLS) measurements were taken on a Nano Zetasizer (Malvern Panalytical Ltd., Malvern, UK). Quantification of Mn and Cu was achieved through an inductively coupled plasma optical emission spectrometer (ICP-OES) (Flexar/NexlON300X, Perkin-Elmer, U.S.A.).

Synthesis of CuSe

CuSe was prepared using a microwave-assisted method. Solutions A and B were separately constituted. For Solution A, SeO_2 (20 mM) was

dissolved in 25 mL of deionized water, followed by the addition of a small quantity of hydrazine hydrate. This mixture was stirred for five minutes to yield Solution A. For Solution B, $CuCl_2 \cdot 2H_2O$ (20 mM) and a minor quantity of PVP were dissolved in 25 mL deionized water and mixed thoroughly for five minutes, resulting in Solution B. Solution A was then incorporated into Solution B, stirring continually for 20 min. Subsequently, the combined solution was heated in a microwave oven at 700 W for three minutes. After cooling to ambient temperature, the solution underwent centrifuge washes with deionized water and ethanol three times, followed by vacuum drying at 60°C overnight to yield the final product, CuSe.

Synthesis of CuSe@PDA

120 mg of pre-synthesized CuSe was dispersed in 40 mL of deionized water. 60 mL of Tris-HCl buffer (pH = 8.5) was subsequently added and the mixture was stirred for 30 min at room temperature. After the addition of 0.4 g of dopamine hydrochloride, the mixture was stirred for another four hours at room temperature. The resulting CuSe@PDA was isolated by centrifugation.

Synthesis of MnFe-LDH

To synthesize MnFe-LDH, 1.5 mM of $MnCl_2 \cdot 4H_2O$ and 0.5 mM of $FeCl_3 \cdot 6H_2O$ were dissolved in 30 mL of deionized water. The solution's pH was adjusted to 13.0 with a 0.2 M NaOH solution and stirred for an additional five minutes. This resultant solution was transferred to a reaction kettle and the reaction was performed at 120 °C for three hours. After naturally cooling to room temperature, the product was washed by centrifugation and finally re-dispersed in deionized water.

Synthesis of CuSe@PDA-MnFe-LDH-PEG [1]

80 mg of CuSe@PDA was first ultrasonically dispersed in 100 mL of distilled water. Subsequently, 10 mg of MnFe-LDH was introduced and the solution was

agitated continuously for 12 h, followed by washing with deionized water. To improve aqueous solubility, 0.1 g of mPEG-SH was incorporated and the mixture was stirred at room temperature for an additional 12 h. The product was then rinsed with deionized water.

Evaluation of POD-mimic activity in CPMF

To evaluate the POD-mimic activity of CPMF, TMB served as the substrates in a reaction with H_2O_2 within a pH 6.0 PBS solution. Following a specific reaction time, the absorbance of the reaction medium was determined using a UV-vis spectrophotometer.

ESR measurements

The generation of ·OH from the reaction of CPMF with H_2O_2 was assessed using DMPO as a spin trapping reagent. A mixture was prepared containing 20 μL CPMF (50 μg/mL), 10 μL DMPO (0.8 M), 20 μL H_2O_2 (0.1 M), and 160 μL PBS (pH = 6.0). This solution was transferred to a capillary tube and situated within the ESR cavity. The ESR spectra were captured at room temperature with a Bruker A300 spectrometer under the following parameters: scan width, 200 G; microwave frequency, 9.873 GHz; microwave power, 2.015 mW, and scan time, 41.9 s.

GSH depletion with CPMF

Various concentrations of CPMF (0, 25, 50, 75, and 100 μg/mL) were combined with GSH (1.0 mM) in a PBS solution at room temperature. Subsequently, 0.2 mM DTNB was added to determine the quantity of SH groups in GSH. The absorbance at 412 nm was recorded after a certain reaction time using a UV-vis spectrophotometer.

Cell culture and cytotoxicity assessment

The 4T1 and HL-7702 cells were cultivated using RPMI 1640 and DMEM mediums respectively, supplemented with 10% fetal bovine serum and 1% penicillin/streptomycin. All cultures were maintained in an incubator at 37 °C under a

humidified atmosphere containing 5% CO_2. The cells were seeded at a density of 10^4 cells per well in 96-well plates and incubated for 24 h under identical conditions. Subsequently, medium solutions containing varying CPMF concentrations (0, 15, 30, 60, 90, and 120 μg/mL) nanoparticles were introduced to 4T1 and HL-7702 cells respectively. The cells were then incubated at 37 °C with 5% CO_2 for an additional 24 hours. Cell viability was subsequently evaluated using the MTT assay.

In vivo experiments

Balb/c female mice, aged between 6 and 8 weeks, were procured from Hunan SJA Laboratory Animal Co., Ltd. (Changsha, China). All animal handling processes adhered to the Animal Ethics Committee guidelines of Guangxi Normal University (Approval No. 202202-002). The mice were maintained under specific-pathogen-free conditions with unrestricted access to standard food and water. All animal studies complied with the guidelines established by the National Regulation of China for Care and Use of Laboratory Animals. Tumor inoculation was performed by subcutaneously injecting 1×10^6 4T1 cells suspended in PBS into the right leg of each Balb/c female mouse.

In vitro and in vivo PA imaging

PA imaging was executed using an iThera Medical's MSOT inVision 256-TF small animal scanner. Transparent 6-mm plastic tubes, commercially obtained, were each filled with either PBS as a control solution or a sample solution and were subsequently secured in the instrument's holder. For in vitro PA evaluations, varying concentrations of CPMF (0, 15, 30, 60, 90, and 120 μg/mL) were prepared and inserted into the associated PA tubes for imaging. For in vivo PA imaging, 4T1 tumor-bearing mice were anesthetized and placed on the MSOT inVision 256-TF small animal scanner. After administration of CPMF (100 μL, 90 μg/mL), PA imaging was conducted at multiple time points (1.0, 4.0, 6.0, 8.0, 10.0, 24.0, and 36.0 h). Whole-body scans were performed in 0.3 mm increments. Following data collection, PA images were reconstructed via a standard inverse projection algorithm.

In evaluating the combined chemokinetic/photothermal cancer treatment efficacy of CPMF in vivo, thirty female tumor-bearing Balb/c mice were randomly allocated into six groups (five mice per group): (i) control group (saline injection); (ii) NIR laser group (1064 nm laser exposure only); (iii) MnFe-LDH group (MnFe-LDH injection only); (iv) CPMF group (CPMF injection only); (v) MnFe-LDH + laser group (MnFe-LDH injection plus 1064 nm laser exposure); and (vi) CPMF + laser group (CPMF injection plus 1064 nm laser exposure). All injected nanomaterials had a volume of 200 μL and a concentration of 90 μg/mL. All groups were treated every other day for 14-day, the frequency of treatment was 7 times during the 14-day treatment period. Tumor temperature and thermographic images were recorded post five-minute laser irradiation (at a power of 1.0 W/cm^2) using an Optris PI infrared camera.

Body weight and tumor size were monitored bi-daily throughout the treatment period. Tumor volume (V) was calculated as V = (a×b^2)/2, where *a* represents the longest dimension and *b* the shortest. After a 14-day treatment period, the mice were euthanized and major tissues, namely heart, liver, spleen, lung, and kidney, were collected for subsequent histological analysis.

The calculation of photothermal transduction efficiency (η)

The photothermal transduction efficiency (η) is calculated as follows:[2]

$$\eta = \frac{hA(T_{max} - T_0) - hA(T_{max,H_2O} - T_0)}{I(1 - 10^{-A_\lambda})} \times 100\% \quad (1)$$

Where h is the heat transfer coefficient. A is the surface area of the sample well. T_{max} representing the equilibrium temperature is 62.8 °C. T_0 representing the ambient temperature is 26.4 °C. $T_{max,H2O}$ representing the maximum steady-state temperature of water is 27.6 °C. A_{1064} representing the absorption intensity of CPMF (90 μg/mL) at 1064 nm is 0.484 (Fig. S14A), and η is the photothermal conversion efficiency.

The thermal time constant should be the same for either heating or cooling of the solution. hA can be determined by applying the linear time data from the cooling

period *vs* –lnθ (Fig. S14B).

$$hA = \frac{m \times C}{K} \tag{2}$$

Where *k* the mass of the sample solution (*m*s) is 0.3 g, and its heat capacity value (*C*) is approximated to be 4.2 J/(g • K). The slope of the linear equation in Fig. S13B (*k*) is 150.87.

$$hA = \frac{0.3 \times 4.2}{150.87} = 0.0835$$

Finally, substituting *hA* value into Equation 1, the η can be calculated as follow:

$$\eta = \frac{0.0835 \times [(62.8 - 26.4) - (27.6 - 26.4)]}{1.0 \times \left(1 - 10^{-0.484}\right)} \times 100\% = 43.7\%$$

Supplementary Figures

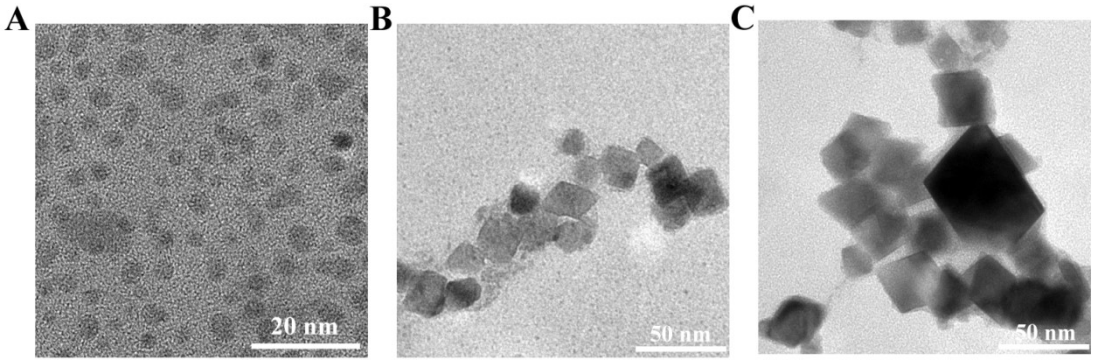

Fig. S1 (A) TEM image of CuSe; (B) TEM image of MnFe-LDH; (C) TEM image of CPMF.

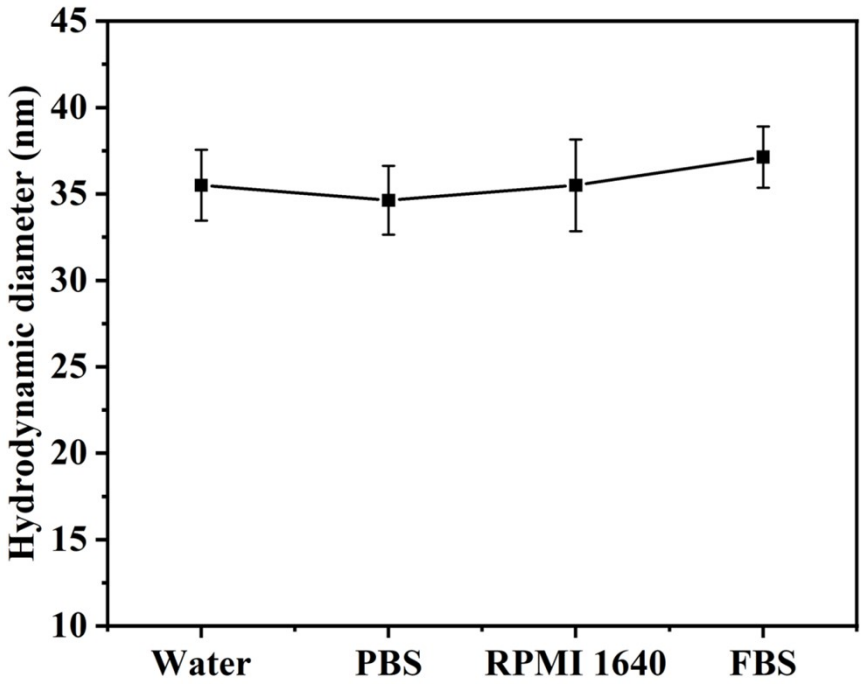

Fig. S2 Hydrodynamic diameters of CPMF in various physiological media (n =3).

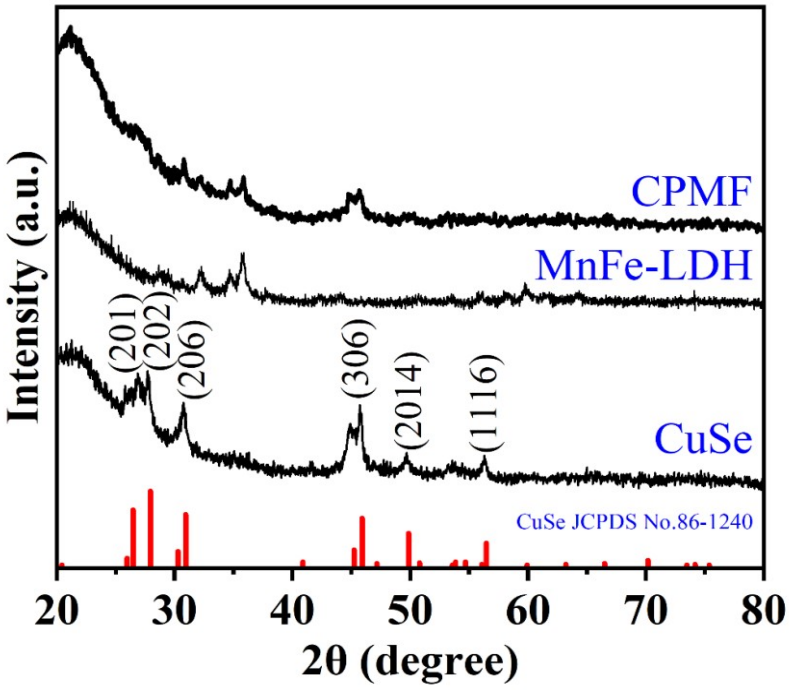

Fig. S3 XRD spectra of as-synthesized CuSe, MnFe-LDH and CPMF.

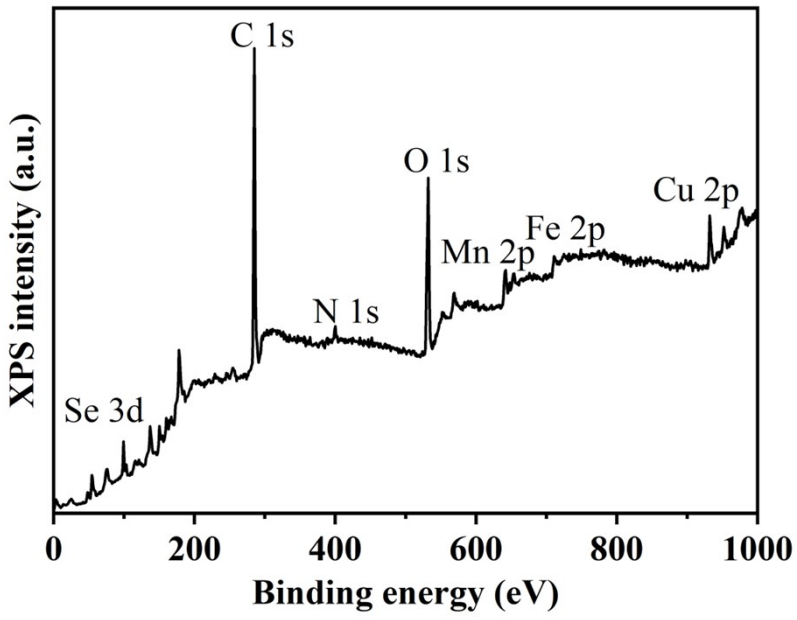

Fig. S4 XPS spectrum of CPMF layered nanosheets.

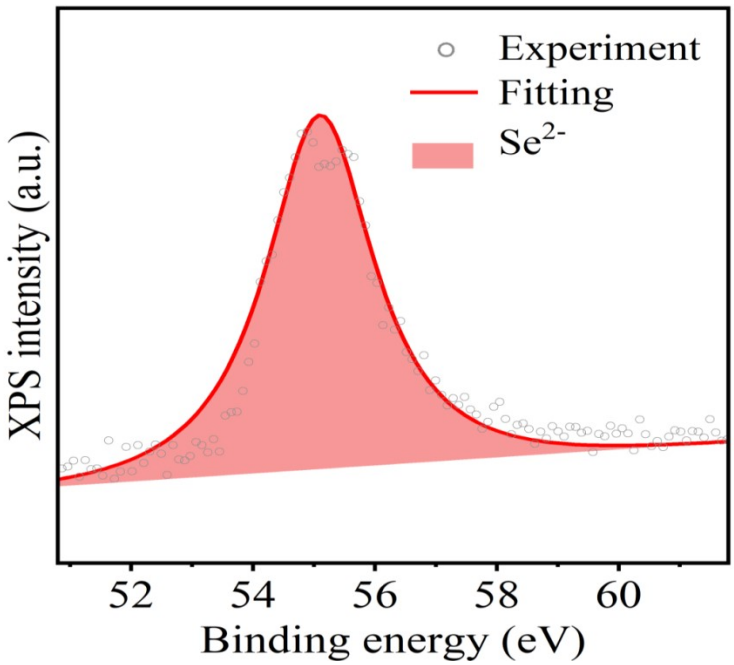

Fig. S5 High-resolution XPS spectrum of Se in CPMF layered nanosheets.

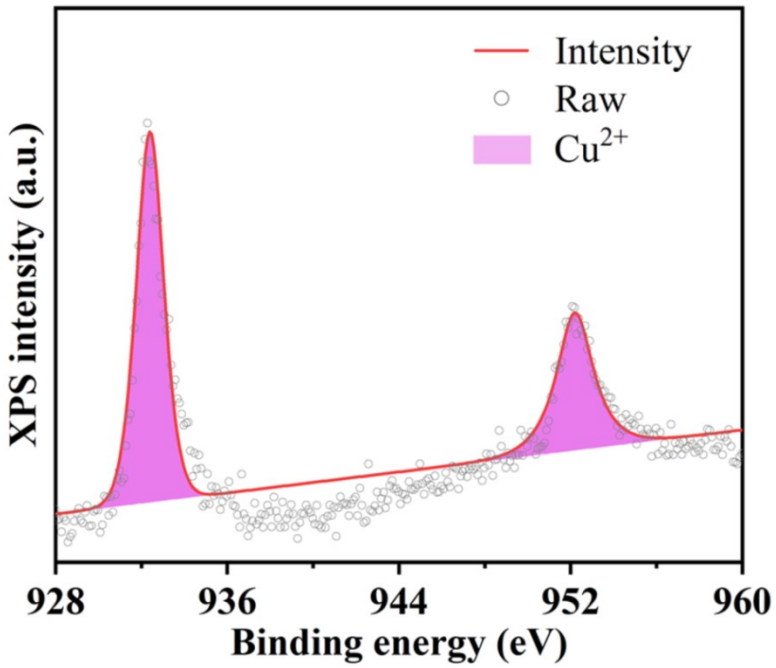

Fig. S6 High-resolution XPS spectrum of Cu in CPMF layered nanosheets.

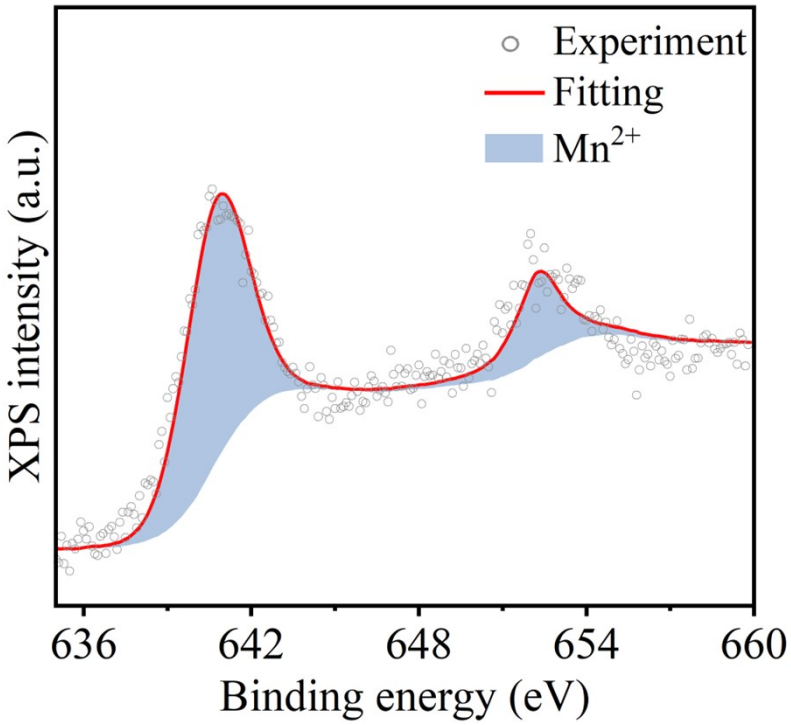

Fig. S7 High-resolution XPS spectrum of Mn in CPMF layered nanosheets.

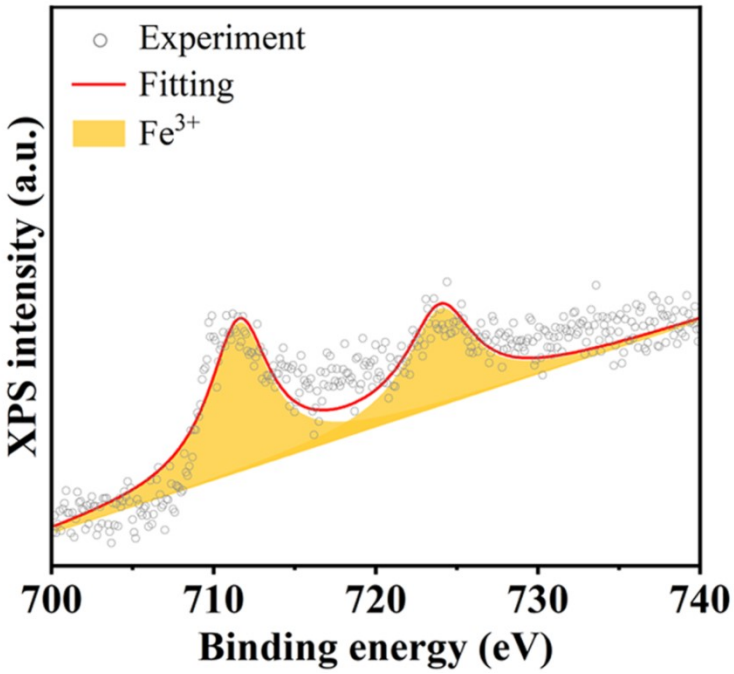

Fig. S8 High-resolution XPS spectrum of Fe in CPMF layered nanosheets.

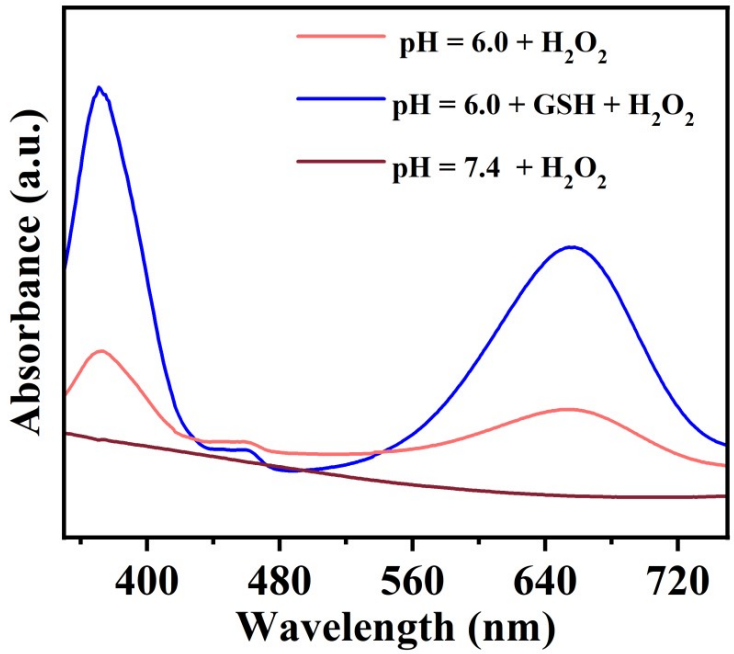

Fig. S9 Absorption spectra of the catalyzed oxidation products of TMB obtained after reaction with CPMF in different conditions.

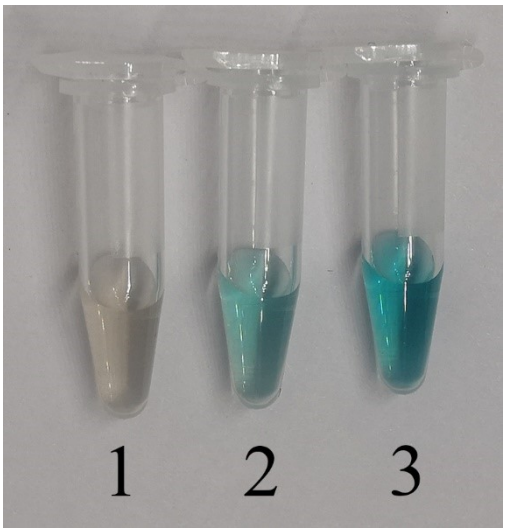

Fig. S10 Photographs following the reaction of different treatments for CPMF with TMB (Group 1: reaction with H_2O_2 only, pH = 7.4; Group 2: reaction with H_2O_2 only, pH = 6.0; Group 3: reaction with GSH and H_2O_2, pH = 6.0).

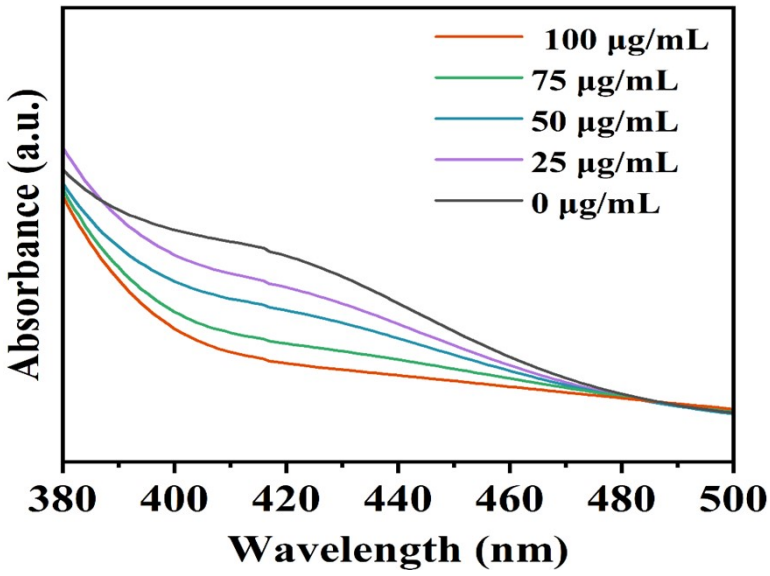

Fig. S11 Absorption curves for DTNB probes after the reaction with different concentrations of CPMF (0, 25, 50, 75 and 100 μg/mL) with GSH.

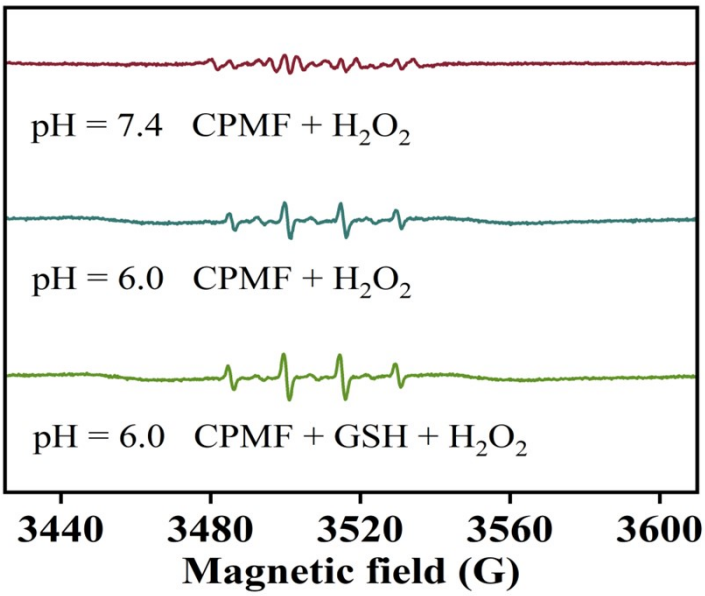

Fig. S12 ESR spectra of ·OH production at different pH values for different treatments of CPMF in the presence of DMPO and H_2O_2.

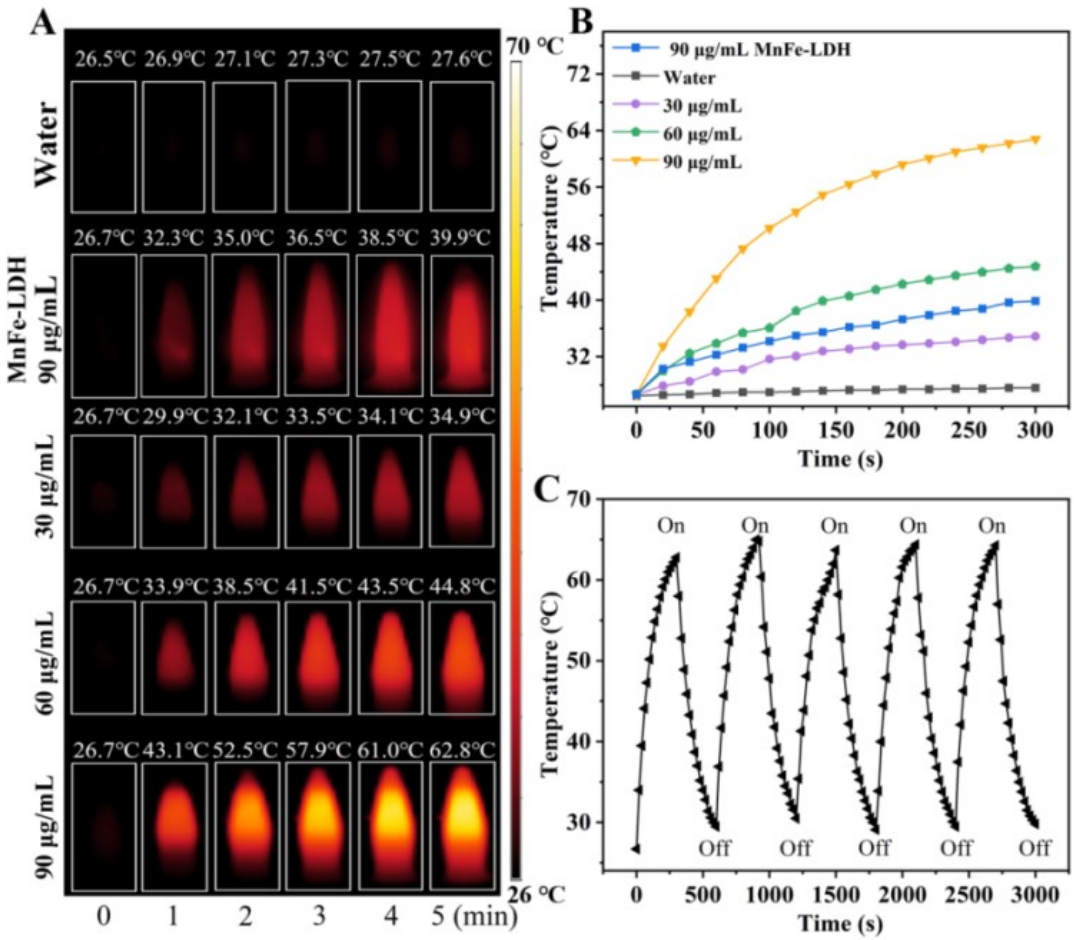

Fig. S13 (A) Infrared thermal images of different concentrations of CPMF and 90 μg/mL of MnFe-LDH. (B) Temperature versus time curves of different concentrations of CPMF and 90 μg/mL of MnFe-LDH irradiated with 1064 nm laser at 1.0 W/cm^2 for 5 min. (C) Heating curves of the conversion cycle of CPMF under 1064 nm laser irradiation (heating for 5 min and cooling for 5 min, for five cycles).

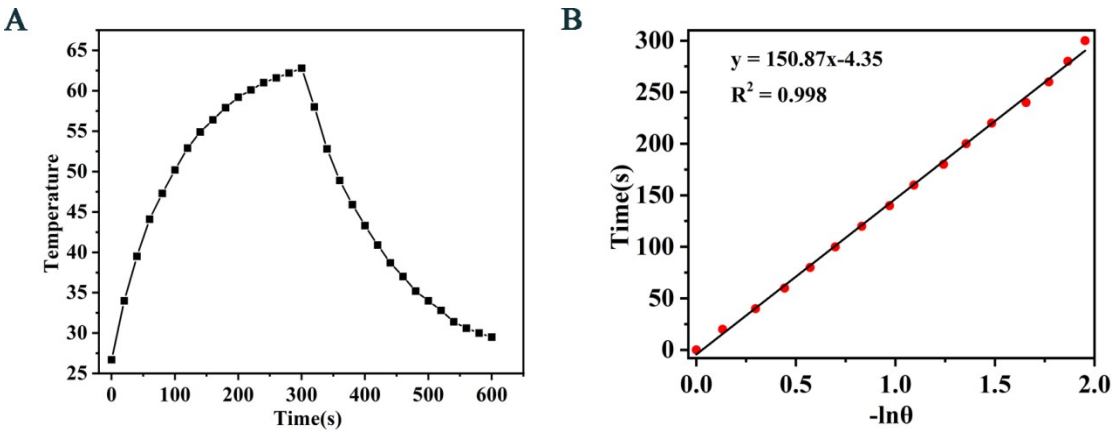

Fig. S14 (A) Photothermal response of CPMF for 5 min with an NIR laser (1064 nm, 1.0 W/cm^2), and then the laser was shut off. The concentration of CPMF is 90 μg/mL. (B) Linear time data versus -lnθ obtained from the cooling period of Fig. S13A).

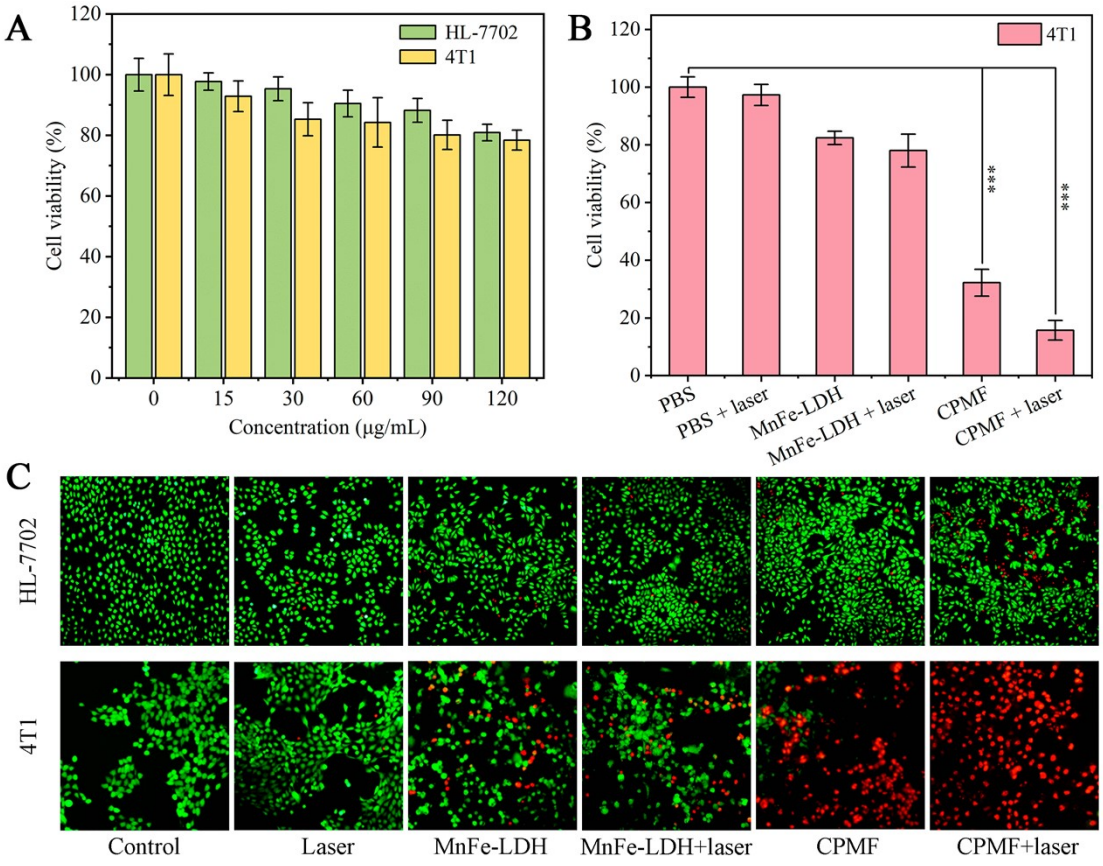

Fig. S15 (A) Cell viability of HL-7702 and 4T1 cells treated with various concentrations CPMF for 24 h. (B) Cell viability of 4T1 cells with different treatments. All data in the graph represent the mean ± SD (n = 3), *P*-values were calculated using ordinary one-way ANOVA, $^{*}p < 0.05$, $^{**}p < 0.01$, $^{***}p < 0.001$. (C) CLSM fluorescence images of live and dead HL7702 and 4T1 cells with calcein-AM/PI double staining in different treatments.

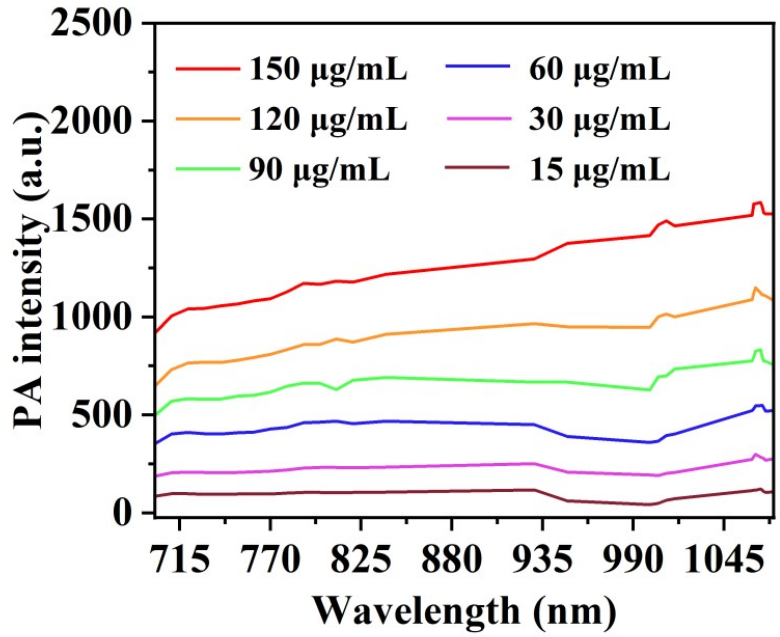

Fig. S16 PA curves for different concentrations of CPMF layered nanosheets.

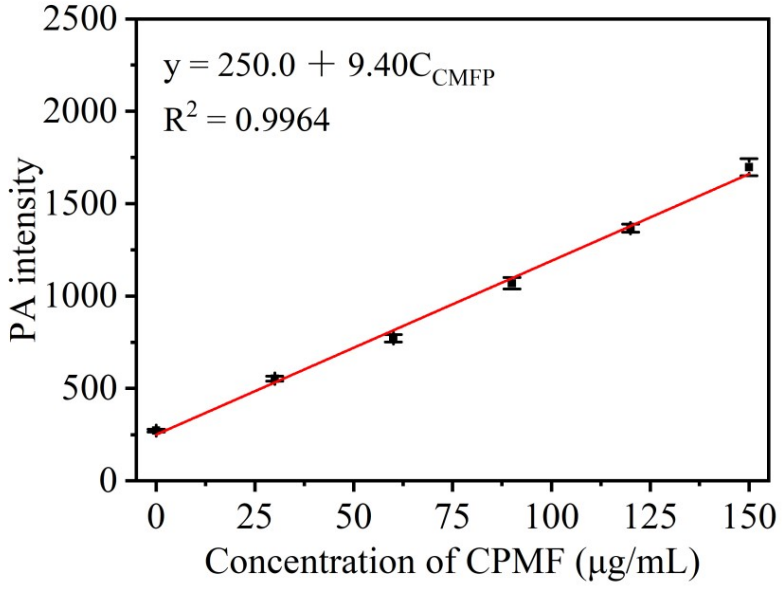

Fig. S17 Standard curve of PA intensity versus CPMF concentration.

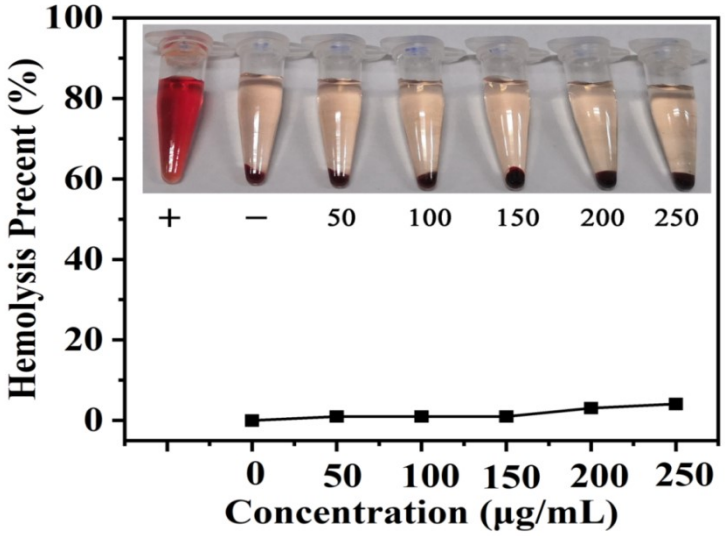

Fig. S18 Hemolytic activity of CPMF with different concentrations after red blood cells (RBCs) incubation for 2 h at 37 ºC.

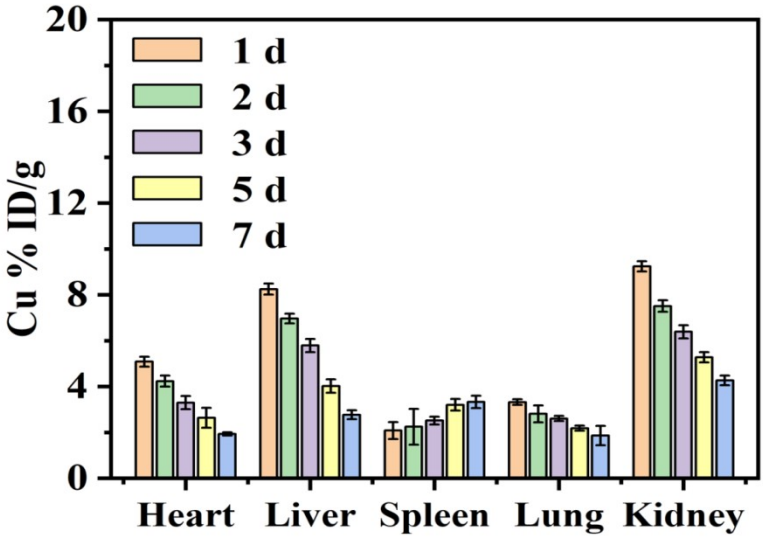

Fig. S19. Biodistribution of Cu in main organs and tumor tissue of 4T1 tumor-bearing mice at different times points after intravenous injecting CPMF.

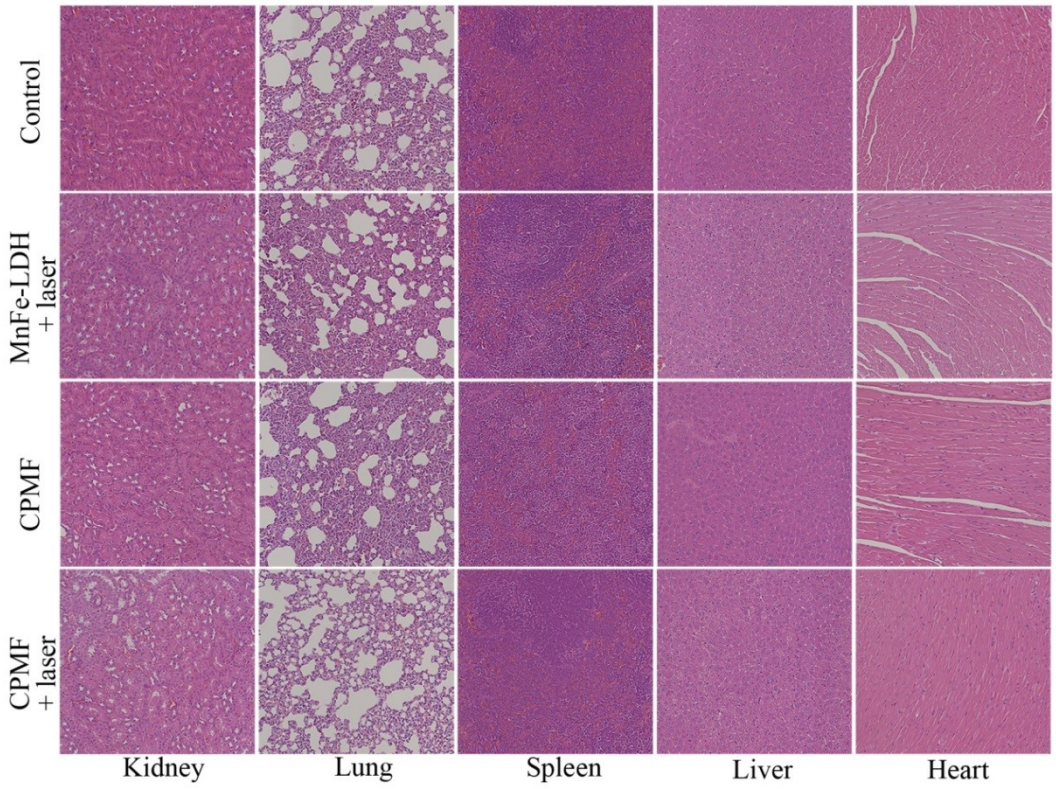

Fig. S20 H&E stained tissues of various organs in Balb/c nude mice harboring the 4T1 tumor xenograft after different treatments.

References:

1. G. Huang, K. L. Zhang, S. Chen, S. H. Li, L. L. Wang, L. P. Wang, R. Liu, J. Gao and H. H. Yang, *J. Mater. Chem. B*, **2017**, *5*, 3629-3633.

2. Y. Liu, K. Ai, J. Liu, M. Deng, Y. He and L. Lu, *Adv. Mater.*, **2013**, *25*, 1353.